

Engineering Notes

ENGINEERING NOTES are short manuscripts describing new developments or important results of a preliminary nature. These Notes cannot exceed 6 manuscript pages and 3 figures; a page of text may be substituted for a figure and vice versa. After informal review by the editors, they may be published within a few months of the date of receipt. Style requirements are the same as for regular contributions (see inside back cover).

Effect of Strake Geometry and Centerbody on the Lift of Swept Wings

Michael P. Schultz* and Karen A. Flack†
United States Naval Academy,
Annapolis, Maryland 21402-5042

Introduction

MODERN fighter/attack aircraft rely on vortex flow to increase lift at moderate to high angle of attack α . Therefore, a great deal of interest exists in understanding and predicting the vortical flow structure generated by swept wings. One form of vortex control uses small geometry modifications (fillets) at the strake-wing junction to alter the vortex dynamics. Fillets are also possible candidates for roll control devices, being deployed symmetrically for enhanced lift and longitudinal control or asymmetrically for lateral-directional control, as discussed by Hebbar et al.¹ Excellent reviews of these vortex control concepts are given by Lamar,² Rao and Campbell,³ and Kern.⁴

Various studies have looked at the effect of fillets on the interaction of the wing and strake vortices. A numerical study by Kern⁴ on a 76/40-deg swept wing indicated that linear and diamond-shaped fillets could increase lift by up to 14% at low α and up to 8% at high α with a small improvement in lift-to-drag ratio. An experimental study on the same wing geometry was conducted in a water tunnel by Hebbar et al.¹ The inclusion of fillets produced a more complicated vortex interaction caused by the formation of additional vortices in the fillet region. Flow visualization indicated a delay in vortex burst for diamond-shaped fillets, with no definitive trend in the vortex response for linear and parabolic-shaped fillets. Another possible benefit of fillets at the strake-wing junction might be a reduction in tail buffet. Impingement of burst vortices on the vertical tails of modern fighter/attack aircraft, referred to as tail buffet, has, in some cases, caused structural fatigue and necessitated replacement of the tails. Ghee et al.⁵ investigated the magnitude and frequency of the tail response to vortex forcing using a matrix of pressure transducers on the vertical tails of a 76/40-deg flat-plate, swept wing. The parabolic fillet created the most tail buffet because this geometry results in a strong vortex system. The discontinuous shape of the diamond-shaped fillet results in a number of vortices resulting in a weaker vortex system that led to the weakest tail buffet.

The primary objective of the present experiment was to investigate the lift characteristics of fillets on a three-dimensional model

and compare the results to a flat-plate model with the same planform. It was also hoped to experimentally validate and quantify the increase in lift as a result of fillets on flat-plate models with the same planform as the three-dimensional model. A secondary objective was to evaluate the effect of a simple centerbody on the lift of flat-plate models with and without fillets as a means for comparison to the full three-dimensional model.

Experimental Apparatus

Wind-Tunnel Facility

Tests were performed in a subsonic wind tunnel at the U.S. Naval Academy. This is a low-turbulence, open-return, closed-jet facility with a test section 79 cm in height, 112 cm in width, and 3.05 m in length. The tunnel uses a 185-kW electric motor controlled with a variable frequency drive and delivers a maximum freestream velocity of about 100 ms⁻¹. Flow management in the settling chamber consists of a high-aspect-ratio honeycomb flow straightener and a series of fine mesh screens. The nozzle contraction ratio is 9.6:1. The resulting freestream turbulence intensity in the test section is 0.06%. The test section is fitted with a six-component, sting-type force balance system. The α of the model can be varied from -35 to $+35$ deg using computer-controlled stepping motors. The data from the sting balance are acquired using a Hewlett-Packard Model 3852, 13-bit, data-acquisition system connected to a PC.

Swept-Wing Models

A baseline swept-wing model and several derivatives were tested in this investigation. The baseline model was a 1:28 scale, three-dimensional model of a modern fighter/attack aircraft. The wing span of the model S was 45.8 cm with a mean aerodynamic chord (MAC) of 14.26 cm and a wing reference area of 592.5 cm². It was constructed of fiberglass-reinforced plastic. Derivatives of this model incorporated linear, parabolic, and diamond-shaped fillets at the strake-wing junctions. The fillets increased the wing area by 1% and were similar to those used by Kern,⁴ Hebbar et al.,¹ and Ghee et al.⁵ on a 76/40-deg flat-plate, swept-wing model. The two remaining models were flat-plate, swept-wing models (Fig. 1a). The first had the same planform as the baseline model. The second had the same planform as the baseline model with the linear fillets. Linear-shaped fillets were selected because they represent a much simpler geometry to fabricate than the diamond or parabolic fillets, and the numerical results of Kern⁴ showed that they can significantly enhance lift at high α . Both flat-plate models were tested with and without the addition of an ogival cylinder centerbody on the top surface. The centerbody was placed at a distance $x/L = 0$ and 0.2 (Fig. 1b). These results are referred to as the forward centerbody and aft centerbody results, respectively. All of the flat-plate models used in the experiments were 7.2 mm thick and were constructed of biaxial carbon fiber skins over a plywood core. The leading and trailing edges of the strake, wing, and tail were sharp, 20-deg beveled with a flat top surface.

Results and Discussion

The tests were conducted at a constant wind-tunnel velocity of 63.5 ms⁻¹ ($Re = 5.8 \times 10^5$ based on MAC). Each model was statically pitched from -10 to $+25$ deg in 1-deg increments on a sting-type six-component force-balance system. Force-balance data were collected at a 60-Hz sampling rate over a 1-min interval. The acquired raw force data were reduced in accordance with the standard

Presented as Paper 2001-2408 at the AIAA 19th Applied Aerodynamics Conference, Anaheim, CA, 11 June 2001; received 19 July 2001; revision received 14 November 2001; accepted for publication 15 November 2001. This material is declared a work of the U.S. Government and is not subject to copyright protection in the United States. Copies of this paper may be made for personal or internal use, on condition that the copier pay the \$10.00 per-copy fee to the Copyright Clearance Center, Inc., 222 Rosewood Drive, Danvers, MA 01923; include the code 0021-8669/02 \$10.00 in correspondence with the CCC.

*Assistant Professor, Ocean Engineering, 590 Holloway Road, M.S. 11D.

†Associate Professor, Mechanical Engineering, Member AIAA.

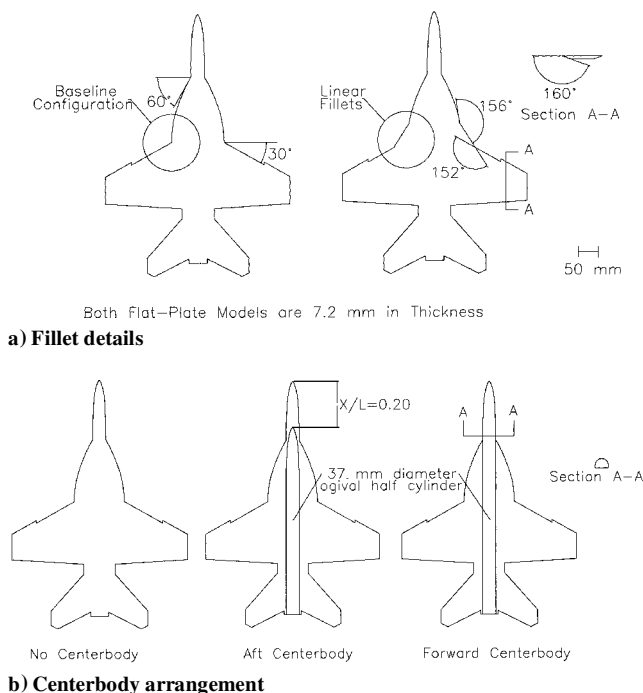


Fig. 1 Plan view of flat-plate models.

procedures outlined in Barlow et al.⁶ This included removal of weight and deflection tares, solid and wake blockage corrections, conversion to force coefficients, wall interference upwash correction, and conversion of force coefficients from body to wind axes.

Precision uncertainty estimates for the resulting mean lift coefficients were made using repeatability tests. Ten replicate pitch sweeps were made on all of the model configurations. The standard error for the mean lift coefficient C_L at each α was calculated. To estimate the 95% precision confidence limits in the mean, its standard error was multiplied by the two-tailed t value ($t = 2.262$) for 9 deg of freedom and significance level of 0.05, as given by Coleman and Steele.⁷ These were combined with the estimates of the bias errors to predict the overall 95% confidence limits for C_L . These were estimated to be less than $\pm 1.5\%$ for all of the models tested.

The lift coefficient results for several of the configurations tested are shown in Fig. 2. The ordinate in the figure was chosen to be $C_L - C_{L_0}$ so that the results from the three-dimensional and flat-plate models could be more easily compared. The lift coefficient at $\alpha = 0$ deg, C_{L_0} , was nearly zero for all of the three-dimensional cases tested and was negative for all of the flat-plate cases because of the beveled edge on the suction side (see Fig. 1a). The centerbody and fillets did not have a significant effect on C_{L_0} . The results in Fig. 2 indicate that within the experimental uncertainty the linear fillet had no significant effect on C_L for the three-dimensional model over the range of α tested. Though not presented here, this was also the case for the diamond and parabolic fillets. These results conflict with the flat-plate studies of Kern⁴ and Hebbar et al.,¹ which both indicated an increase in lift with the inclusion of fillets. The three-dimensional model results seem to indicate that there are distinct differences in the vortex interaction and breakdown between the flat-plate and three-dimensional model. The results for the flat-plate model show a significant increase in lift in the moderate-to-high α range with linear fillets as compared to the no-fillets case. The increase in C_L ranged from 5.6 to 12.9% and averaged 9.4% for $\alpha = +10$ to $+20$ deg. The increase ranged from 2.5 to 6.1% and averaged 3.7% for $\alpha = +20$ to $+25$ deg. These results, although on a different planform, show similar trends as seen in the numerical study of Kern⁴ on a flat-plate, 76/40-deg swept wing.

It was hypothesized that the differences in lift obtained for the three-dimensional model as compared to the flat-plate model was caused by a fuselage effect. Results for the flat-plate model with and without a centerbody are also shown in Fig. 2. The results for

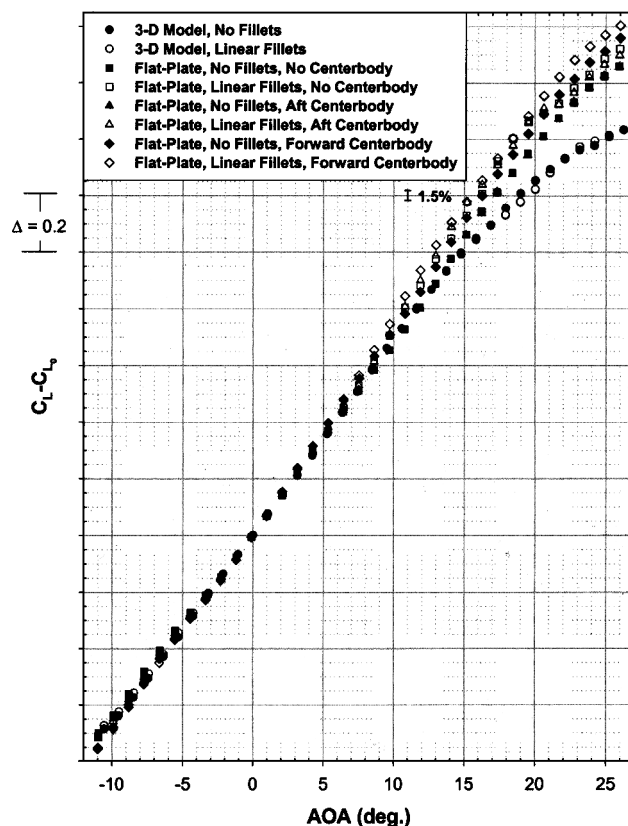


Fig. 2 Lift coefficient results for all model types with and without linear fillets.

the flat-plate model with a centerbody show a significant increase in lift in the moderate-to-high α range with linear fillets as compared to the no-fillets case. The increase in C_L ranged from 7.8 to 12.5% and averaged 9.9% at $\alpha = +10$ to $+20$ deg for the aft centerbody case. The increase ranged from 2.1 to 7.3% and averaged 3.3% at $\alpha = +20$ to $+25$ deg. For the forward centerbody case the increase in C_L ranged from 4.2 to 8.9% and averaged 6.0% at $\alpha = +10$ to $+20$ deg. The increase ranged from 2.2 to 4.2% and averaged 3.4% at $\alpha = +20$ to $+25$ deg. The aft centerbody had no significant effect on the lift for the flat-plate model, with or without linear fillets, as these results agree within their uncertainty with those taken without a centerbody. The forward centerbody results, with or without linear fillets, indicate an increase in C_L over both the aft centerbody and no centerbody cases.

The results for the three-dimensional model and the flat-plate models given in Fig. 2 show significant differences. Although this is not surprising in itself, the trends shown for the fillets vs no-fillets cases are not in agreement. As stated before, the fillets increased the lift on the flat-plate models and did not on the three-dimensional model. This illustrates that caution should be exercised when attempting to apply findings from flat-plate models to three-dimensional models and full-scale aircraft. In the present study the addition of a simple centerbody did not yield any better agreement between the model type. Further research into size, geometry, and placement of the centerbody should be undertaken to better address the ability of a flat-plate model to predict the trends in performance of a three-dimensional model.

Conclusions

The following conclusions can be made from the present experimental investigation:

- 1) Linear fillets placed at the strake-wing junction on a flat-plate, swept-wing model led to a significant increase in C_L at moderate-to-high α ($+10$ to $+25$ deg).
- 2) Linear, parabolic, and diamond fillets at the strake-wing junction on the three-dimensional model had little effect on C_L over the entire α range (-10 to $+25$ deg).

3) A centerbody on the flat-plate models had little effect on the lift coefficient and did not produce better agreement with the three-dimensional model than the flat-plate model alone.

4) Caution should be exercised when attempting to apply results and overall trends from flat-plate, swept-wing models to three-dimensional models and full-scale aircraft.

Acknowledgments

The authors gratefully acknowledge the financial support of the Office of Naval Research for the U.S. Naval Academy postdoctoral research program and the technical support of NAVAIR.

References

- ¹Hebbar, S. K., Platzer, M. F., and Alkhozam, A. M., "Experimental Study of Vortex Flow Control on Double-Delta Wings Using Fillets," *Journal of Aircraft*, Vol. 33, No. 4, 1996, pp. 743–751.
- ²Lamar, J. E., "Nonlinear Lift Control at High Speed and High Angle of Attack Using Vortex Flow Technology," *Special Course on Fundamentals of Fighter Aircraft Design*, AGARD-R-740, Neuilly-sur-Seine Cedex, France, Oct. 1987, pp. 4.1–4.23.
- ³Rao, D. M., and Campbell, J. F., "Vortical Flow Management Techniques," *Progress in Aerospace Sciences*, Vol. 24, No. 3, 1987, pp. 173–224.
- ⁴Kern, S., "Vortex Flow Control Using Fillets on a Double-Delta Wing," *Journal of Aircraft*, Vol. 30, No. 6, 1993, pp. 818–825.
- ⁵Ghee, T. A., Gonzalez, H. A., and Findlay, D. B., "Experimental Investigation of Vortex-Tail Interaction on a 76/40 Degree Double-Delta Wing," AIAA Paper 99-3159, June 1999.
- ⁶Barlow, J. B., Rae, W. H., and Pope, A., *Low-Speed Wind Tunnel Testing*, 3rd ed., Wiley, New York, 1999, pp. 234–427.
- ⁷Coleman, H. W., and Steele, W. G., "Engineering Application of Experimental Uncertainty Analysis," *AIAA Journal*, Vol. 33, No. 10, 1995, pp. 1888–1896.

Assessment of Simultaneous Perturbation Stochastic Approximation Method for Wing Design Optimization

X. Q. Xing* and M. Damodaran†

Singapore—Massachusetts Institute of Technology
Alliance (SMA), Singapore 119260, Republic of Singapore
and

Nanyang Technological University,
Singapore 639798, Republic of Singapore

Introduction

THE need for addressing optimization problems that are characterized by the presence of a large number of design variables, complex constraints, and discrete design parameter values exists in many fields including engineering design. A variety of local and global optimization algorithms have been developed for addressing such problems. Besides deterministic methods, stochastic methods such as genetic algorithm (GA) and simulated annealing (SA) algorithm have recently found applications in many practical engineering design optimization problems. These algorithms are easily implemented in robust computer codes as compared with deterministic methods because they do not depend on direct gradient

information, which most deterministic methods do. However, SA and GA methods require a large number of function evaluations and relatively longer computation time than deterministic methods, especially in the case of complex design problems. Although the use of parallel GA and parallel SA as outlined in Wang and Damodaran¹ offers a way to reduce the large computational time, an attractive alternative to SA and GA could be the simultaneous perturbation stochastic approximation (SPSA) method described in Spall.² The SPSA method has been applied to numerous difficult multivariate optimization problems in many diverse areas such as statistical parameter estimation, feedback control, simulation-based optimization, signal and image processing, and experimental design. The essential feature of SPSA, which accounts for its power and relative ease of implementation, is the underlying gradient approximation, which requires only two measurements of the objective function regardless of the dimensions of the optimization problem. This feature allows for a significant decrease in the cost of optimization, especially for problems with a large number of variables to be optimized.

The aim of this Note is to compare performance of SPSA with SA and GA and to explore any advantages that SPSA might offer to overcome the large computational efforts of SA and GA when applied to wing-design problems. These methods are briefly outlined following the statement of the wing-design optimization problem, which will form the application problem to assess and compare the performance of SPSA in relation to SA and GA.

Wing-Design Problem

The application concerns the design of wing shape such that the aerodynamic efficiency of the wing or the lift L to drag D ratio reaches a maximum value during cruise with the wing weight acting as a constraint, that is, the goal is to determine the wing geometry by either minimizing D/L or maximizing L/D with the wing weight as a constraint. The D/L ratio can be formulated in detail using the analytic formulas for aerodynamic analysis as defined in Raymer.³ The lift L is defined as $L = C_L q S$, where $q = \frac{1}{2} \rho V^2$ is the dynamic pressure, ρ is the density of air, V is the flight speed, $C_L = C_{L\alpha} \alpha$ is the lift coefficient where α is the angle of attack and $C_{L\alpha} = 2\pi A_R / [2 + \sqrt{4 + (A_R \beta / \eta)^2 (1 + \tan^2 \lambda / \beta^2)}]$ is the lift curve slope. In the expression for lift curve slope, $A_R (= b^2/S)$ is the wing aspect ratio, where b is the wing span, λ is the wing sweep angle, η (value of which lies in the range 0.95–1.0) is the airfoil efficiency factor, $\beta = 1 - M^2$ is the compressibility factor, and M is the Mach number. The total drag is defined as $D = C_D q S$, where the total drag coefficient is $C_D = C_{Di} + C_{D0}$, which consists of the induced drag coefficient $C_{Di} = C_L^2 / (\pi A_R e)$ and the zero-lift drag coefficient $C_{D0} = C_f F Q$. In these expressions $e = 4.61(1 - 0.045 A_R^{0.68})(\cos \lambda)^{0.15} - 3.1$ is the wing planform efficiency factor, $C_f = 0.455 / [(\log_{10} Re)^{2.58} (1 + 0.144 M^2)^{0.65}]$ is the surface skin-friction coefficient, which is a function of the Reynolds number Re , $F = \{1 + [0.6/(x/c)_m](t/c) + 100(t/c)^4\} [1.34 M^{0.18} (\cos \lambda)^{0.28}]$ in which t/c is the airfoil thickness-to-chord ratio, $(x/c)_m$ is the chord-wise location of the maximum thickness-to-chord ratio, taken as 0.3 in the present study, and Q is a factor accounting for interference effects on drag taken as 1.0 in the present study. The weight of the wing (in pounds) is $W_{\text{wing}} = 0.0106 (W_{\text{dg}} N_z)^{0.5} S^{0.622} A_R^{0.75} (t/c)^{-0.4} (\cos \lambda)^{-1}$, where W_{dg} is the design gross weight in pounds and N_z is the ultimate load factor, which is assumed to be 13.5 for subsonic flow.

The design variables for the wing design optimization, that is, α , b , c , λ , and W_{wing} , represent the angle of attack, wing span, mean aerodynamic chord, sweep angle, and wing weight, respectively. The objective function to be optimized is $F(X) = D/L$ and is defined as follows:

$$\text{Minimize } F(X) \quad (1)$$

subject to six constraints on the design variables defined as follows:

$$\begin{aligned} 1.0 \text{ deg} \leq \alpha \leq 10.0 \text{ deg}, & \quad 10.0 \leq b \leq 50.0 \\ 3.5 \leq c \leq 10.0, & \quad 0.0 \text{ deg} \leq \lambda \leq 35.0 \text{ deg} \\ 0.5 \leq A_R \leq 15.0, & \quad W_{\text{wing}} \leq 2473 \text{ (lb)} \end{aligned} \quad (2)$$

Received 7 September 2001; revision received 17 September 2001; accepted for publication 30 December 2001. Copyright © 2002 by the American Institute of Aeronautics and Astronautics, Inc. All rights reserved. Copies of this paper may be made for personal or internal use, on condition that the copier pay the \$10.00 per-copy fee to the Copyright Clearance Center, Inc., 222 Rosewood Drive, Danvers, MA 01923; include the code 0021-8669/02 \$10.00 in correspondence with the CCC.

*SMA Research Fellow, 50 Nanyang Avenue.

†SMA Faculty Fellow; Associate Professor, School of Mechanical and Production Engineering, 50 Nanyang Avenue. Associate Fellow AIAA.